AGU PUBLICATIONS

JGR

Journal of Geophysical Research: Atmospheres

RESEARCH ARTICLE
10.1002/2013JD020515

Key Points:
- Spatial data products can be used to estimate soil respiration (R_s)
- Root-zone soil moisture can be used to estimate R_s
- Land surface temperature correlated well with soil temperature

Correspondence to:
N. Huang,
huangni@radi.ac.cn

Citation:
Huang, N., L. Gu, and Z. Niu (2014), Estimating soil respiration using spatial data products: A case study in a deciduous broadleaf forest in the Midwest USA, *J. Geophys. Res. Atmos.*, *119*, 6393–6408, doi:10.1002/2013JD020515.

Received 5 JUL 2013
Accepted 31 JAN 2014
Accepted article online 5 FEB 2014
Published online 10 JUN 2014

Estimating soil respiration using spatial data products: A case study in a deciduous broadleaf forest in the Midwest USA

Ni Huang[1], Lianhong Gu[2], and Zheng Niu[1]

[1]State Key Laboratory of Remote Sensing Science, Institute of Remote Sensing and Digital Earth, Chinese Academy of Sciences, Beijing, China, [2]Environmental Sciences Division, Oak Ridge National Laboratory, Oak Ridge, Tennessee, USA

Abstract This study aimed to investigate the potential of spatially distributed data products in estimating soil respiration (R_s), including land surface temperature (LST) and spectral vegetation index from the Moderate Resolution Imaging Spectroradiometer (MODIS) and root zone soil moisture derived from the assimilation of the NASA Advanced Microwave Scanning Radiometer-EOS and a land surface model, at a deciduous broadleaf forest site in the Midwest USA. Several statistical models were used to examine the dependencies of R_s on these spatial data products, and accuracy of these models was compared to the models based on in situ measurements. The models based on mean LST (i.e., averaging nighttime and daytime LST from MODIS) and root zone soil moisture explained 82% and 72% of seasonal variations in R_s for spring and winter dormant periods, respectively. In the growing season, the models depending on mean LST, root zone soil moisture, and photosynthesis-related enhanced vegetation index showed comparable accuracy with the models entirely based on in situ measured data, except for the midgrowing period. Drought stress led to a relatively low explanation capacity for the R_s model based on spatial data products during the midgrowing period. However, this model still explained 76% of temporal dynamics of R_s over the midgrowing period. Our results suggested that simple models based entirely on spatial data products have the potential to estimate R_s at the temperate deciduous forest site. The conclusions drawn from the present study provided valuable information for large-scale estimates of R_s in temperate deciduous forest ecosystems.

1. Introduction

Soil respiration (R_s) is a major component of CO_2 exchange between terrestrial ecosystems and the atmosphere [*Bahn et al.*, 2008; *Davidson et al.*, 2006; *Ryan and Law*, 2005; *Vargas et al.*, 2011]. R_s can also be used as an ecological indicator of ecosystem functioning [*Oyonarte et al.*, 2012]. Thus, accurate R_s modeling is required to assess carbon budgets of terrestrial ecosystems [*Richardson et al.*, 2006] and understand the effect of global warming on R_s [*von Deimling et al.*, 2012].

R_s is determined largely by a number of biotic and abiotic variables [*Amos et al.*, 2005; *Reichstein et al.*, 2003]. Regression analysis using abiotic variables such as soil temperature, soil water content, or both as predictors [*Davidson et al.*, 1998; *Gaumont-Guay et al.*, 2006; *Lloyd and Taylor*, 1994] has been a classical approach in modeling R_s. In addition, the close coupling between canopy photosynthesis and R_s can make the photosynthate supply become another key determinant of the soil surface CO_2 flux [*Högberg et al.*, 2001; *Kuzyakov and Richkovaw*, 2010; *Moyano et al.*, 2007; *Tang et al.*, 2005a; *Vargas et al.*, 2010]. Therefore, many empirical relationships have been established between field measurements of R_s and soil temperature, soil water content, and photosynthesis-related factors [*Arkebauer et al.*, 2009; *Amos et al.*, 2005; *Han et al.*, 2007; *Liu et al.*, 2006]. However, most of these established relationships only used data measured at the local scale. To obtain R_s at regional, continental, or global scales, significant efforts are needed to use the spatially distributed data for R_s estimation.

To date, remote sensing is used as a major tool for estimating the spatial distribution of carbon balance components, such as gross primary productivity (GPP), net primary productivity, and net ecosystem exchange (NEE) [*Kimball et al.*, 2009; *Peng and Gitelson*, 2011; *Running et al.*, 2000; *Xiao et al.*, 2004]. However, R_s estimation based on remote sensing data remains unclear. Current archives and the availability of satellite data have allowed the possibility of using the remotely sensed data for R_s estimation, such as land surface temperature (LST) and spectral vegetation indices (VIs). LST from remote sensing is possible as a predictor of R_s because of LST's close relationships with the physiological activity of plants and various temperature-related variables [*Mostovoy et al.*, 2006; *Vogt et al.*, 1997; *Zhang et al.*, 2011], which are important determinants of R_s. Greenness VIs not only provide measures of the amount or condition of vegetation within a pixel but also are good indicators of plant photosynthesis [*Gitelson et al.*, 2006; *Rahman et al.*, 2005; *Sims et al.*, 2006; *Wu et al.*, 2010; *Wylie et al.*, 2003]. Thus, VIs may be used to model R_s due to their possible relationships with substrate supply to R_s. LST and surface reflectance products from the Moderate Resolution Imaging Spectroradiometer (MODIS) are increasingly being used to study various ecosystem processes. Moreover, both products have been cross compared or validated over a widely distributed set of locations and time periods [*Fang et al.*, 2004; *Hulley and Hook*, 2009; *Liang et al.*, 2002; *Moncet et al.*, 2011; *Wan*, 2008].

Soil moisture greatly determines the temporal and spatial changes of R_s by affecting the activity of microbes and enzymes and regulating photosynthetic substrate supply and oxygen availability [*Balogh et al.*, 2011; *Cook and Orchard*, 2008; *Jassal et al.*, 2008; *Li et al.*, 2008]. However, despite the importance of soil moisture, accurate assessment is difficult because of strong spatial and temporal variability in topography, soil type, and land use [*Cosh et al.*, 2004; *Famiglietti et al.*, 2008; *Verstraeten et al.*, 2006]. The accuracy of soil moisture estimation from remotely sensed passive microwave observations varies greatly over different land cover types because of signal attenuation by vegetation [*Bolten et al.*, 2003] and is significantly degraded over areas of vegetation water content that is greater than approximately 5 kg m^{-2} [*Njoku and Chan*, 2006]. Thus, the application of microwave remote sensing in estimating soil moisture over forest areas is limited by the effect of high-vegetation water content. However, remote sensing data, when combined with a land surface model, could provide estimates of soil moisture with higher spatial and temporal resolutions and less error than either remotely sensed data or model simulation separately [*Houser et al.*, 1998; *Huang et al.*, 2008]. Integrating surface soil moisture retrievals from the NASA Advanced Microwave Scanning Radiometer–EOS (AMSR-E) into a modified Palmer soil moisture model provides reliable estimation of root zone soil moisture and has been successfully used at regional scale [*Bolten et al.*, 2010].

Previous studies conducted in various types of forest ecosystems have reported a considerable challenge in deriving spatial patterns of soil respiration because of changes in soil temperature, moisture, and substrate supply [*Davidson et al.*, 1998; *Högberg et al.*, 2001; *Gaumont-Guay et al.*, 2006]. At large spatial scales, these factors affecting soil respiration are difficult to observe with in situ measurements due to their large spatial and temporal variability in forest ecosystems. Thus, the application of spatial data products in modeling soil respiration will greatly facilitate estimation of soil respiration over a large spatial scale. The primary objective of this study was to determine if the spatial data products previously mentioned (i.e., LST, VIs, and root zone soil moisture) allow for the estimation of R_s at a deciduous broadleaf forest site. As vegetation phenology at the study site may have a great impact on R_s, we first clarified the main driving factors for R_s variations during growing and nongrowing seasons. Then, we separately modeled seasonal R_s using different statistical models for each phenology stage and examined the feasibility of these R_s models driven by spatial data products at the deciduous forest site.

2. Materials and Methods

2.1. Study Site

The Missouri Ozark AmeriFlux site (38.7441°N and 92.2°W, 219 m) is located in central Missouri, USA. The vegetation type is a temperate deciduous broadleaf forest, dominated by second-growth upland oak-hickory forests [*Pallardy et al.*, 1988]. Major tree species include white oak (*Quercus alba*, *Quercus muehlenbergii*, and *Quercus stellata*), red oak (*Quercus velutina*, *Quercus rubra*, *Quercus shumardii*, and *Quercus imbricaria*), Fraxinus (*Fraxinus americana* and *Fraxinus quadrangulata*), Carya (*Carya ovata*, *Carya cordiformis*, *Carya tomentosa* and *Carya texana*), and *Acer saccharum*. The average rooting depth at this site is over 1 m. Root dry mass decreased exponentially with the increase of soil depth, and approximately 90% root system mass concentrated at the depth of 0 cm to 40 cm (data not shown). The canopy height is approximately 24 m. Soils are mainly Weller silt with rocky thin soil covering. The soil depth varies spatially. At some places, soil depth can be as deep as 2 m. At other locations, soil depth may be just 0.5 m. The climate is warm, humid, and continental with mean July temperature at 25.2°C. Annual mean precipitation is about 940 mm, and annual mean temperature is about 13.5°C. Droughts commonly occur between July and September. *Gu et al.* [2006] provide detailed descriptions of the study site.

Table 1. Vegetation Indices Calculated From MODIS 8 Day Surface Reflectance Product at the Temperate Deciduous Forest Site[a]

Vegetation Index	Formulation	Reference
Normalized difference vegetation index	$\mathrm{NDVI} = \frac{\rho_{\mathrm{nir}} - \rho_{\mathrm{red}}}{\rho_{\mathrm{nir}} + \rho_{\mathrm{red}}}$	*Rouse et al.* [1974]; *Gamon et al.* [1995]
Enhanced vegetation index	$\mathrm{EVI} = 2.5 \times \frac{\rho_{\mathrm{nir}} - \rho_{\mathrm{red}}}{\rho_{\mathrm{nir}} + (6 \times \rho_{\mathrm{red}} - 7.5 \times \rho_{\mathrm{blue}}) + 1}$	*Huete et al.* [2002]
Green chlorophyll index	$CI_{\mathrm{green}} = \frac{\rho_{\mathrm{nir}}}{\rho_{\mathrm{green}}} - 1$	*Gitelson et al.* [2005]

[a]Reflectance of green, blue, red, and near-infrared (NIR) band in MOD09A1 product are ρ_{green}, ρ_{blue}, ρ_{red}, and ρ_{nir}, respectively.

2.2. Soil Respiration, Soil Temperature, and Soil Moisture Measurements

Continuous hourly measurements of R_s, soil temperature, and soil moisture were from the Missouri Ozark AmeriFlux site in 2004 to 2007 (http://ameriflux.ornl.gov/). R_s was measured with eight automated soil chambers [*Edwards and Riggs*, 2003]. The installments of the eight soil chambers consider the spatial heterogeneity (such as soils and vegetation); thus, data from these chambers can be averaged to produce representative efflux data set for the site. Sampling at one chamber took 7 min to 8 min so that a sampling cycle of eight chambers was about 1 h. The resulted time series was at hourly time step with only a few measurement gaps because of freezing tube in winter, instrument failure, and site work. Moreover, the hourly mean R_s should be considered as a spatial average rather than a temporal average.

Soil temperature and soil moisture were continuously measured near the automated chamber system at multiple depths in the deciduous forest site. Half-hourly soil temperature was measured at depths of 2, 4, 8, 16, 32, 64, and 128 cm using the Atmospheric Turbulence and Diffusion Division Probe with YSI Thermistors. Soil moisture was measured at depths of 10, 20, 30, 40, 60, and 100 cm using the Delta–T PR1/6 Profiler capacitance probe. The measurements of soil temperature and moisture were actually performed at different locations at the study site. They appeared fairly homogeneous from varying locations. Thus, we can use these soil temperature and moisture profiles measured near the automated chamber system to represent their values at the observation scale of the flux tower.

To conform to the 8 day period of MODIS data, the 8 day samples of R_s, soil temperature, and soil moisture at different depths were averaged and the means were used in this study. Also, note that the in situ measured data include all days (both sunny and cloudy), whereas the MODIS data include only clear days. Thus, short-term (hours to days) variability has been removed, and this analysis looks only at long-term seasonal variability. Vegetation greenness remains basically constant over 1 week [*Sims et al.*, 2006], and the major patterns of remotely sensed land surface temperature are consistent with measured surface temperature at a weekly scale [*Benali et al.*, 2012; *Jin and Dickenson*, 2010]. Therefore, although only data from sunny days were used from MODIS and all data from in situ measurements were used, this methodology probably has little influence on the results.

2.3. Spectral Vegetation Indices Calculation

MODIS 8 day surface reflectance product (MOD09A1, 500 m) at the study site were downloaded (http://ladsweb.nascom.nasa.gov/data/search.html) to calculate VIs for GPP estimation. Each MOD09A1 pixel contains the best possible observation during an 8 day period as selected based on high observation coverage, low view angle, the absence of clouds or cloud shadow, and aerosol loading. Based on the geolocation information (latitude and longitude) of the study site, the pixel containing the site from the MOD09A1 product was extracted. The same data processing was also applied to the following spatial data products (i.e., MODIS LST, root zone soil moisture, and MODIS phenology products). Table 1 shows the three VIs (i.e., normalized difference vegetation index (NDVI), enhanced vegetation index (EVI), and green chlorophyll index (CI_{green})) calculated from the surface reflectance product. Under ideal conditions, changes in vegetation index (VI) time series indicate changes in vegetation conditions. However, disturbances in these time series are always observed, which are caused by cloud contamination, atmospheric variability, and bidirectional effects. The Savitzky-Golay filter efficiently reduces noises in the VI time series caused primarily by cloud contamination and atmospheric variability [*Chen et al.*, 2004; *Savitzky and Golay*, 1964]. In this study, a Savitzky-Golay filter was used to obtain high-quality VI time series.

Table 2. The Phenological Periods Defined by MODIS Phenology Product (MCD12Q2) at the Temperate Deciduous Forest Site (Units: Day of Year)[a]

Phenology Periods	2004	2005	2006	2007
Spring dormant period	*1–73*	1–71	1–72	1–63
Early growing period	*74–154*	72–135	73–143	64–157
Midgrowing period	155–191	136–271	144–300	158–200
Late-growing period	192–323	272–325	301–322	201–340
Winter dormant period	324–365	326–365	323–365	341–365

[a]Italics mark means that the data during the spring dormant period and early growing period of 2004 are not used in our analysis, because there is no ground observation data during the two periods at the temperate deciduous forest site.

2.4. Land Surface Temperature Data Acquisition

MODIS 8 day LST product (MOD11A2 from Terra MODIS) with 1000 m spatial resolution was downloaded at the study site (http://ladsweb.nascom.nasa.gov/data/search.html). The MOD11A2 product is composed from the daily 1 km LST product and stored on a 1 km Sinusoidal grid as the average values of clear-sky LSTs during an 8 day period. We used only data described as good data quality in the data quality layer of this MOD11A2 product. We averaged daytime and nighttime LST (mean LST) from the MOD11A2 for each 8 day period, and the mean LST was used for the following analysis.

2.5. Root Zone Soil Moisture Data Acquisition

The root zone soil moisture product (http://reverb.echo.nasa.gov/reverb/) is derived from the assimilation of Land Parameter Retrieval Model/AMSR-E/NASA EOS Aqua surface soil moisture retrievals into a two-layer Palmer water balance model, using a one-dimensional, 30-member ensemble Kalman filter. Root zone soil moisture is defined as the two-layer Palmer water balance model predicted soil moisture. The depth of the root zone depends on the available water capacity (AWC) which is calculated using soil texture, depth to bedrock, and soil type derived from the Food and Agriculture Organization (FAO) digital soil map of the world available from the FAO at http://www.fao.org/ag/agl/lwdms.stm#cd1. The range of root zone is typically from 50 cm to 290 cm, depending on the AWC for the region of interest. Detailed descriptions of the method can be found in *Bolten et al.* [2010]. The data set with global coverage covers the period from June 2002 to December 2010 at a spatial resolution of 25 km and a temporal resolution of 1 day. Eight day averaged root zone soil moisture was used in this study. For this analysis, our aim was to see if the root zone soil moisture product can be used as a surrogate of in situ measured soil moisture for R_s estimation. We did not have the aim or possibility to modify this product.

2.6. Phenological Data Acquisition

In this study, MODIS phenology product (MCD12Q2, 500 m) was used to divide phenological phases for data analysis (http://ladsweb.nascom.nasa.gov/data/search.html). MCD12Q2 characterizes vegetation growth cycles using four transition dates estimated from time series of MODIS EVI data: (1) greenup: the date of onset of EVI increase; (2) maturity: the date of onset of EVI maximum; (3) senescence: the date of onset of EVI decrease; and (4) dormancy: the date of onset of EVI minimum [*Ganguly et al.*, 2010]. Using the four transition dates as a basis for separating phenological periods, we partitioned the entire study period into five phenological periods (Table 2), namely, spring dormant period, early growing period, midgrowing period, late-growing period, and winter dormant period.

2.7. Plant Photosynthesis Data Acquisition

GPP, which quantitatively represents plant photosynthesis, was acquired from America Fluxnet (http://public.ornl.gov/ameriflux/). GPP values were obtained by summing NEE and ecosystem respiration (R_e) with eddy covariance measurements at the study site. Daytime ecosystem respiration (R_e) is estimated from night NEE-temperature relationship. Nighttime NEE-temperature relationship could be problematic because of insufficient turbulent air mixing during nights which produces gaps in eddy covariance measurement. Marginal distribution sampling method is used for gap filling [*Reichstein et al.*, 2005]. Incident photosynthetically active radiation (PAR_{in}) was also measured at the eddy covariance tower.

Data acquisition would be simpler and more direct if we could estimate GPP using spectral VI. Earlier studies have shown good relationships between VIs (e.g., NDVI, EVI, and CI_{green}) and vegetation productivity when the data were integrated over the growing season [*Gitelson et al.*, 2006; *Rahman et al.*, 2005; *Sims et al.*, 2006; *Wylie et al.*, 2003]. In this study, we examined the relationships between simple greenness VIs and GPP and used the VI that best correlated with GPP to estimate R_s. In addition, short-term fluctuations of environmental stresses (e.g., photosynthetically active radiation, temperature, humidity, soil moisture, etc.) could induce extreme variations in GPP, whereas the VIs representing vegetation greenness will fail to detect a decrease in GPP related to the types of stressors mentioned. The 8 day averaged GPP was used for our analysis, which removed the effects of short-term (minutes to hours) variability in environmental factors to some extent. However, for comparison, the relationships between GPP and the combination of VI and PAR_{in} (i.e., VI × PAR_{in}) [*Peng and Gitelson*, 2011] or the combination of VI and LST (the temperature and greenness model (i.e., TG model)) [*Sims et al.*, 2008] were analyzed.

2.8. Methods for Soil Respiration Estimation

Various climate conditions have been found to control seasonal variability of R_s, of which soil temperature and soil moisture are often the most influential. The relationship between R_s and soil temperature is usually modeled by a simple exponential function [*Gaumont-Guay et al.*, 2006; *Liu et al.*, 2006; *Lloyd and Taylor*, 1994]. A general form of this function is

$$R_s = B_0 e^{B_1 T} \tag{1}$$

However, in this temperate deciduous forest, soil moisture was also observed to be an important factor affecting seasonal patterns of R_s [*Gu et al.*, 2008]. We therefore used a model with soil temperature and soil moisture as driving variables to model seasonal R_s. Similar models have been used previously in Mediterranean ecosystems [*Tang et al.*, 2005b; *Vargas and Allen*, 2008].

$$R_s = B_0 e^{B_1 T} e^{B_2\theta + B_3\theta^2} \tag{2}$$

Moreover, we observed significant effects of plant photosynthesis (i.e., gross primary production (GPP)) on R_s during the growing season at the study site. In addition to equation (2), which adequately described R_s during nongrowing season, we developed a model (equation (3)) simulating R_s at growing season. In equation (3), we simply assumed that one part of R_s is purely driven by biotic factors (e.g., GPP) and the other by abiotic ones (e.g., soil temperature and moisture), similar to the report of *Migliavacca et al.* [2011].

$$R_s = B_0 e^{B_1 T} e^{B_2\theta + B_3\theta^2} + B_4 GPP + B_5 \tag{3}$$

where R_s (μmol CO_2 m^{-2} s^{-1}) is the soil respiration, T (°C) the soil temperature, and θ ($m^3 m^{-3}$) the volumetric soil moisture. The quadratic-type form of θ indicates that soil moisture has two opposite effects on R_s. B_0, B_1, B_2, B_3, B_4, and B_5 are the model parameters. These parameters can vary with seasonal variations in decomposition rates of soil labile carbon [*Gu et al.*, 2004]. To reduce this influence, we first partitioned the entire study period into five different phenological periods and separately modeled R_s using equations (1) to (3) for each phenological stage.

To test the feasibility of using spatial data products in estimating R_s, we used remotely sensed land surface temperature and spectral vegetation index as a proxy indicator of soil temperature and GPP, respectively, and root zone soil moisture, from assimilation of AMSR-E and a land surface model, as a surrogate of soil moisture to estimate R_s based on equations (1) to (3).

2.9. Statistical Analysis

To quantify the temporal variability in R_s, soil temperature, soil moisture, and GPP for each phenological period, the coefficient of variation (CV) was calculated as follows:

$$\mathrm{CV} = \text{standard deviation}/\text{mean} \times 100\% \tag{4}$$

The Marquardt–Levenberg algorithm was used to determine the model parameters. Model accuracy and performance were evaluated by three statistics: coefficient of determination (R^2), root-mean-square error (RMSE), and Akaike's information criterion (AIC) [*Richardson et al.*, 2006]. The best model had the highest R^2 and lowest RMSE and AIC based on the three metrics.

To clarify the main factors affecting R_s during different phenological periods, we first examined the performances of the models (equations (1) to (3)) using in situ measured soil temperature, soil moisture, and GPP as driving factors. Then, to see if the spatial data products (i.e., mean LST, root zone soil moisture and VIs) could be used to estimate R_s, we examined the relationships between these data products and in situ measured biotic or

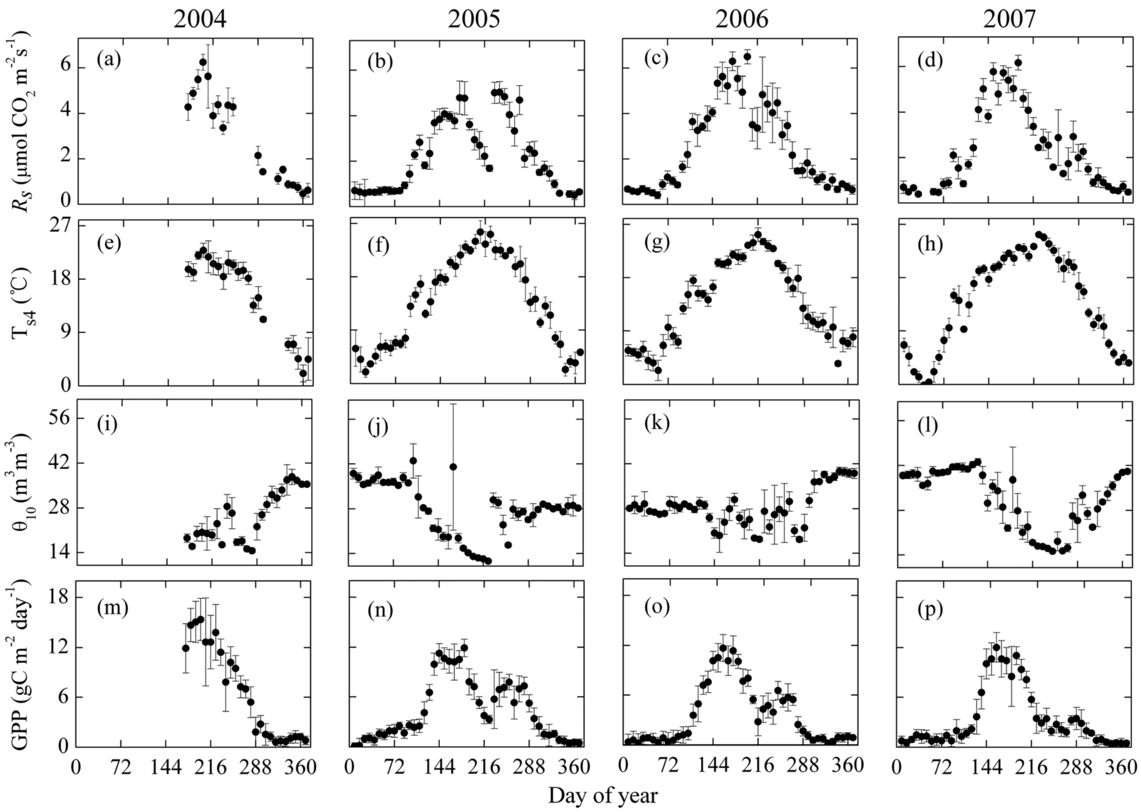

Figure 1. Seasonal patterns of (a–d) soil respiration (R_s), (e–h) soil temperature at 4 cm depth (T_{s4}), (i–l) soil moisture at 10 cm depth (θ_{10}), and (m–p) gross primary production (GPP) at the Missouri Ozark AmeriFlux site in 2004–2007. All data are 8 day mean and showed in 8 day interval. Error bars represent 1 standard error.

abiotic factors (i.e., soil temperature, soil moisture, and GPP). On this basis, we analyzed the performances of the models entirely driven by the spatial data products.

In this study, multicollinearity diagnostics were conducted after the establishment of soil respiration models. Multicollinearity diagnostics serve to detect collinearity among the predictive variables used for estimating soil respiration (equations (2) and (3)). The presence of collinearity will cause the model parameters to differ greatly from their true values, even to the point of having incorrect signs. Therefore, the collinearity statistics need to be examined when the predictive variables are highly intercorrelated. To determine if multicollinearity existed in our data set, Pearson correlation and variance inflation factor (VIF) were evaluated on all the predictive variables for estimating soil respiration in five different phenological periods. Generally, the lower the Pearson correlation coefficient and VIF are, the weaker is the multicollinearity problem among the predictive variables. All statistical analyses were conducted using the Statistical Package for the Social Sciences (SPSS) 13.0 (SPSS, Chicago, IL, USA).

3. Results

3.1. Seasonal Variation of Soil Respiration

Similar to the seasonal variations of soil temperature and GPP, R_s showed an obvious seasonal pattern at the deciduous forest site during 2004 to 2007 (Figure 1). The maximum 8 day mean R_s usually occurred at the midgrowing period and corresponded to the maximum values of soil temperature and GPP (Figure 1 and Table 3). However, in response to the seasonal drought at the midgrowing season of 2005, R_s decreased dramatically with a significant decrease in soil moisture (Figure 1). Mean R_s at the deciduous forest site ranged between 0.64 and 4.14 μmol CO_2 m^{-2} s^{-1} at the five different phenological periods (Table 3). Furthermore, R_s showed obviously larger temporal variations at early and late-growing periods than at other phenological periods with a CV of 54% and 57%, respectively. During nongrowing season (i.e., spring or winter dormant periods), the CV of R_s was small and coincident with the small CV of soil moisture (Table 3).

Table 3. Seasonal Characteristics of Soil Respiration (R_s, μmol CO_2 m^{-2} s^{-1}), Soil Temperature at 4 cm Depth (T_{s4}, °C), Soil Moisture at 10 cm Depth (θ_{10}, $m^3 m^{-3}$), and Gross Primary Production (GPP, gC m^{-2} day^{-1}) at the Temperate Deciduous Forest Site From 2004 to 2007 for Five Different Phenological Periods

	Mean	Minimum	Maximum	Coefficient of Variation (CV, %)
		Spring Dormant Period		
R_s	0.64	0.39	1.16	27
T_{s4}	4.93	1.28	9.59	43
θ_{10}	32.92	26.22	40.16	16
		Early Growing Period		
R_s	2.44	0.70	5.02	54
T_{s4}	13.69	6.70	20.04	29
θ_{10}	32.65	20.32	42.95	20
GPP	4.14	0.50	12.00	83
		Midgrowing Period		
R_s	4.14	1.44	6.48	33
T_{s4}	20.83	10.65	25.57	16
θ_{10}	23.23	11.57	41.03	29
GPP	7.32	0.55	14.32	45
		Late-Growing Period		
R_s	2.45	0.72	6.25	57
T_{s4}	16.73	6.85	25.27	33
θ_{10}	24.33	15.13	38.64	26
GPP	4.39	0.56	14.38	88
		Winter Dormant Period		
R_s	0.71	0.47	1.07	23
T_{s4}	5.84	3.49	9.62	31
θ_{10}	35.33	28.22	40.10	12

For the modeling of R_s, we used soil temperature at 4 cm depth (T_{s4}) and soil moisture at 10 cm depth (θ_{10}), as the soil temperature or soil moisture at other depths were not able to explain more of the seasonal variances in R_s. During the spring and winter dormant periods, the best model to explain temporal variations in R_s at the deciduous forest site, based on the AIC, was a model depending on T_{s4} alone. However, addition of θ_{10} to the model slightly increased the R^2 value and reduced the RMSE (Table 4), suggesting that soil moisture also had an influence on R_s at this deciduous forest site in the nongrowing season.

For the early growing period, the model depending on T_{s4} explained most of the seasonal variations in R_s, and a further addition of θ_{10} and GPP only slightly increased the explanation power (Table 4). By contrast, soil temperature played a less important role in regulating seasonal variations in R_s than soil moisture at the midgrowing and late-growing periods, which indicated that soil moisture was an important factor affecting R_s during the two phenological periods. Furthermore, the addition of GPP to the model considering soil temperature and soil moisture greatly increased the R^2 value and reduced the RMSE and AIC (Table 4) demonstrated that plant photosynthesis also had an important influence on R_s at the deciduous forest site during the midgrowing and late-growing periods. The importance of GPP in the modeling of R_s was particularly evident for the midgrowing period with an obvious increase of R^2 from 0.53 to 0.90 ($p < 0.0001$, Table 4). Overall, the best model to explain seasonal variations in R_s during the midgrowing and late-growing periods at the deciduous forest site was a function of soil temperature, soil moisture, and GPP when comparing all three model performance indicators (R^2, RMSE, and AIC, Table 4).

3.2. Spatial Data Used for Soil Respiration Estimation

3.2.1. Land Surface Temperature Data From MODIS

To clarify if the mean LST from MODIS was able to represent soil temperature for R_s estimation at our study site, we analyzed the seasonal changes in mean LST and soil temperature measured at different depths (Figure 2). We did not show the measured soil temperature at all depths, because the seasonal trends shown in Figure 2 can be broadly extended to the other depths of soil temperature. Both the mean LST and the in situ measured soil temperature at four different depths showed strong seasonality. The mean LST and the in situ measured soil temperature reached a maximum in the middle of the growing season and were low at the nongrowing season.

Table 4. Results of Regression Analysis Relating Soil Respiration to Soil Temperature, Soil Water Content, Gross Primary Production, and Their Corresponding Variables From Spatial Data Products at the Deciduous Forest Site[a]

Models and Equations	Spring Dormant Period			Early Growing Period			Midgrowing Period			Late-Growing Period			Winter Dormant Period		
	R^2	RMSE	AIC	R^2	RMSE	AIC	R^2	RMSE	AIC	R^2	RMSE	AIC	R^2	RMSE	AIC
Soil Temperature															
$R_s = B_0 e^{B_1 T_{s4}}$	0.86	0.06	−39.60	0.84	0.52	−8.23	0.15[b]	1.24	14.27	0.44	1.03	6.87	0.71	0.09	−26.14
Soil Temperature and Soil Moisture															
$R_s = B_0 e^{B_1 T_{s4}} e^{B_2 \theta_{10} + B_3 \theta_{10}^2}$	0.87	0.06	−35.85	0.90	0.41	−9.52	0.53	0.92	6.89	0.86	0.51	−9.67	0.78	0.07	−23.85
Soil Temperature, Soil Moisture, and Gross Primary Production															
$R_s = B_0 e^{B_1 T_{s4}} e^{B_2 \theta_{10} + B_3 \theta_{10}^2} + B_4 GPP + B_5$				0.92	0.35	−8.52	0.90	0.42	−19.65	0.93	0.36	−16.62			
Land Surface Temperature															
$R_s = B_0 e^{B_1 \mathrm{LST\text{-}mean}}$	0.81	0.07	−37.30	0.86	0.49	−9.61	0.16[b]	1.23	14.02	0.41	1.06	7.61	0.66	0.09	−25.03
Land Surface Temperature and Root Zone Soil Moisture															
$R_s = B_0 e^{B_1 \mathrm{LST\text{-}mean}} e^{B_2 \theta_r + B_3 \theta_r^2}$	0.82	0.07	−33.02	0.87	0.47	−6.62	0.75	0.67	−5.67	0.90	0.44	−13.96	0.72	0.08	−22.32
Land Surface Temperature, Root Zone Soil Moisture, and Spectral Vegetation Index															
$R_s = B_0 e^{B_1 \mathrm{LST\text{-}mean}} e^{B_2 \theta_r + B_3 \theta_r^2} + B_4 \mathrm{EVI} + B_5$				0.96	0.27	−14.53	0.76	0.65	−2.64	0.90	0.43	−11.13			

[a] R^2 is the coefficient of determination, RMSE (μmol CO_2 m^{-2} s^{-1}) is the root-mean-square error, and AIC is the Akaik's information criterion. T_{s4} is soil temperature at 4 cm depth (°C), θ_{10} is volumetric soil moisture (m^3 m^{-3}) at 10 cm depth, GPP is gross primary production (gC m^{-2} day^{-1}), and R_s is soil respiration (μmol CO_2 m^{-2} s^{-1}). LST-mean is the averaged daytime and nighttime land surface temperature (LST) from Terra MODIS (°C), θ_r is the root zone soil moisture (m^3 m^{-3}), and EVI is enhanced vegetation index for estimating GPP. The other quantities are model parameters describing the assumed functional dependency of the quantities. All relationships are statistically significant at $p < 0.0001$(***), except the R^2 marked by "b" which means that the statistical analysis is significant at 0.01 level.

Moreover, soil temperature at greater depth showed obvious time hysteresis compared with the soil temperature close to the surface (Figure 2). Throughout the study period, mean LST best captured the seasonal change of surface soil temperature (i.e., T_{s4}), while mean LST exhibited larger values and variations than T_{s4} during the midgrowing period of 2004 to 2007. Furthermore, mean LST showed the best correlation with T_{s4} ($R^2 = 0.97$, $p < 0.0001$) than soil temperature at other depths (Figure 3).

3.2.2. Root Zone Soil Moisture

The in situ measured soil moisture and modeled root zone soil moisture during the study period at the deciduous forest site were shown in Figure 2. As expected, high-frequency variations were seen in the time series of in situ measured soil moisture at 10, 20, and 30 cm depths and low-frequency variations at 100 cm depths. Overall, root zone soil moisture showed approximate values and a similar variation pattern with soil moisture at intermediary depths (i.e., 40 cm and 60 cm, Figure 2). Linear regression analysis also showed that root zone soil moisture closely tracked the seasonal dynamics of soil moisture at 40 cm depth with a coefficient of determination of 0.73 ($p < 0.0001$). With the depth increase or decrease, the correlations between in situ measured soil moisture and root zone soil moisture greatly reduced (Figure 4).

For the root zone soil moisture, the assimilation of AMSR-E surface soil moisture retrievals into the Palmer model improves the root zone soil moisture estimation, especially in bare soil and low-vegetation-covered regions. At densely vegetated areas (i.e., forest), AMSR-E performance is not expected to be optimal because of the vegetation density limitations. Thus, over these regions, the soil moisture estimates will rely more on the precipitation and temperature data than on the assimilated remotely sensed soil moisture product. Our study site is a forest area, good relationship between root zone soil moisture and soil moisture measured at

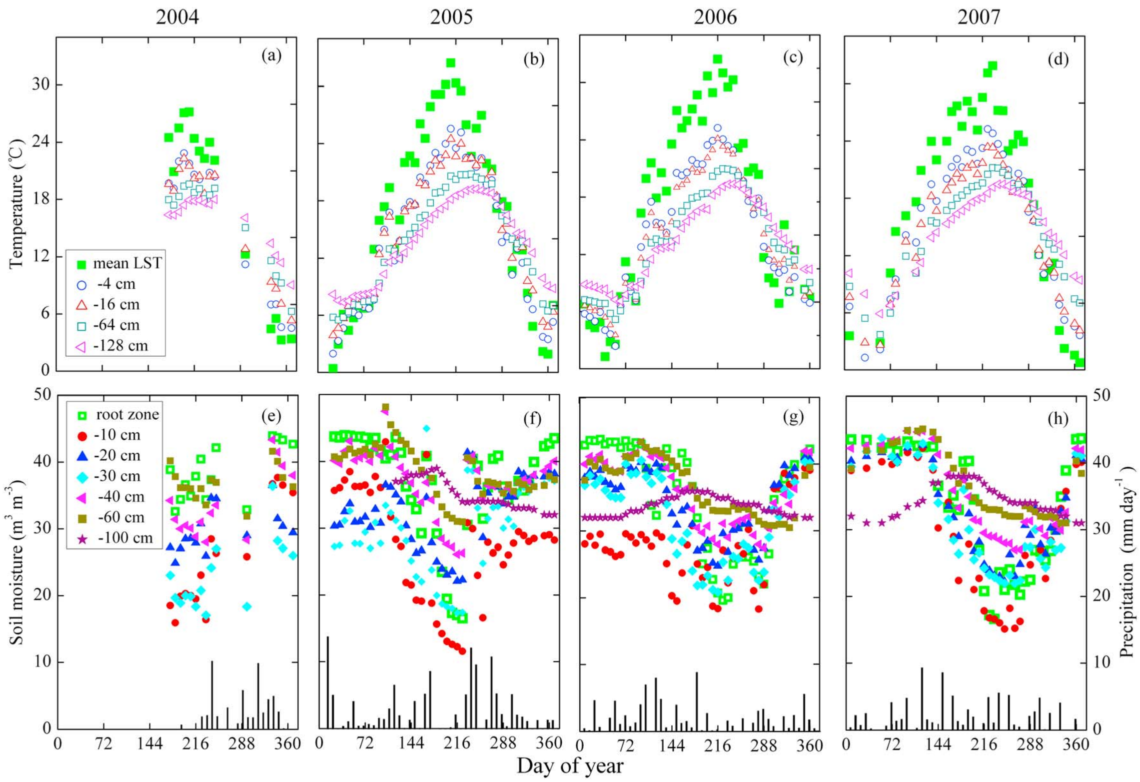

Figure 2. Seasonal courses of 8 day mean land surface temperature (mean LST): (a–d) soil temperature at 4 cm, 16 cm, 64 cm, and 128 cm depths and (e–h) soil moisture at root zone 10 cm, 20 cm, 30 cm, 40 cm, 60 cm, and 100 cm depths, precipitation (Figures 2e–2h, right axis) at the temperate deciduous forest site in 2004–2007. Only the mean for each 8 day period is presented for clarity.

40 cm depth ($R^2 = 0.73$) was observed. This good relationship indicated that the root zone depth predicted by the Palmer model at the study site was about 40 cm, which was reasonable considering that most root system mass concentrates at the depth of 0 cm to 40 cm and the range of root zone depth in the root zone soil moisture product typically ranges from 50 cm to 290 cm (from private communication with the producers of root zone soil moisture product).

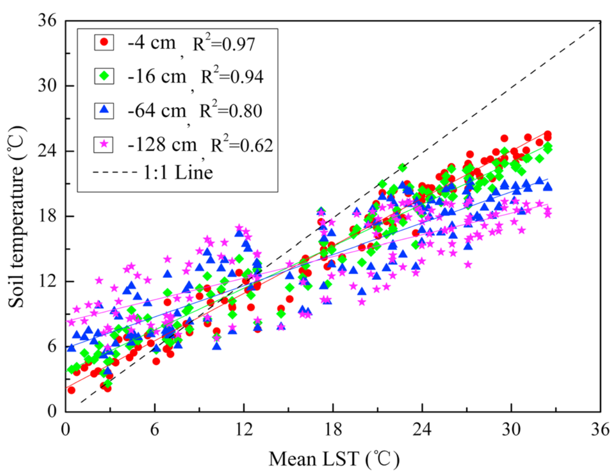

Figure 3. Relationships between mean LST and in situ measured soil temperature at the 4 cm, 16 cm, 64 cm and 128 cm depths at the deciduous forests site in 2004–2007. Mean LST is the averaged daytime and nighttime land surface temperature from Terra MODIS for each 8 day period. All relationships were statistically significant at $p < 0.0001$ ($n = 136$).

3.2.3. Spectral Vegetation Index

Throughout the growing season of 2004 to 2007 at the deciduous forest site, EVI showed slightly better relationship with GPP than NDVI and CI_{green} (Table 5). Moreover, combining VI and PAR_{in} did not provide obvious higher accuracy for estimating GPP than using VIs alone. Integrating LST and EVI (TG model) [*Sims et al.*, 2008] produced better correlation with GPP than either the EVI alone or the combination of EVI and PAR_{in}, but the

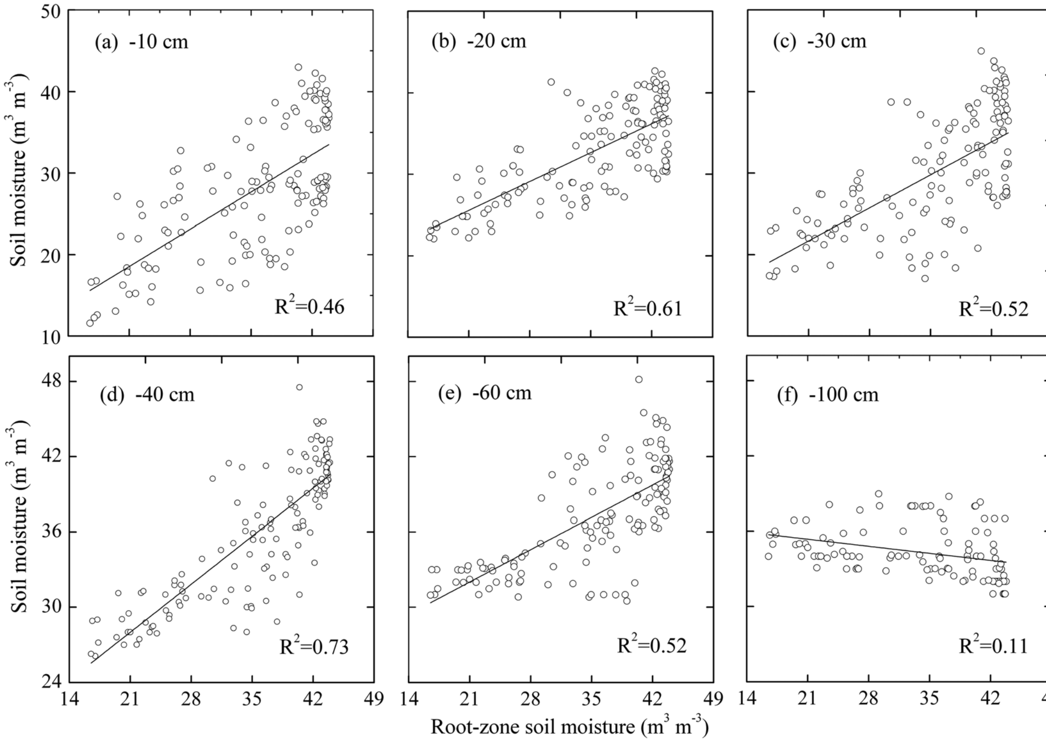

Figure 4. (a–f) Relationships between root zone soil moisture and in situ measured soil moisture at 10 cm, 20 cm, 30 cm, 40 cm, 60 cm, and 100 cm depths at the temperate deciduous forests site in 2004–2007. All relationships were statistically significant at $p < 0.0001$ ($n = 136$).

improvement was small (Table 5). Thus, we selected EVI as a surrogate of GPP for R_s estimation as the single VI was simpler than using the combination of LST and VI (i.e., TG model) [*Sims et al.*, 2008].

3.3. Estimating Soil Respiration Using Spatial Data Products

When comparing all three model performance indicators (R^2, RMSE, and AIC), the models based on mean LST or the combination of mean LST and root zone soil moisture showed similar performances to the model entirely based on in situ measured T_{s4} or the combination of T_{s4} and θ_{10} at the deciduous forest site during spring and winter dormant periods (Table 4). In the early growing period, compared with the model depending on the mean LST alone, inclusion of root zone soil moisture to model R_s did not obviously improve the fitting accuracy. Further addition of the plant photosynthesis-related VI (i.e., EVI) explained an additional 9% of the seasonal variation in R_s at the study site (Table 4). Thus, based on the spatial data products, the best model to describe seasonal pattern of R_s in the early growing period was the model based on mean LST, root zone soil moisture, and EVI (Table 4).

During the midgrowing and late-growing periods, the model based on both the mean LST and root zone soil moisture showed much better explanation capacity for the seasonal variations in R_s than the model based on

Table 5. Determination Coefficients (R^2) and Root-Mean-Square Error (RMSE) of Linear Relationships Between Gross Primary Production (GPP) and Variables Used for GPP Estimation at the Temperate Deciduous Forest Site During the Growing Season of 2004–2007[a]

	NDVI	EVI	CI_{green}	NDVI × PAR_{in}	EVI × PAR_{in}	CI_{green} × PAR_{in}	TG Model
R^2	0.66	0.71	0.70	0.66	0.72	0.73	0.75
RMSE	2.45	2.26	2.28	2.45	2.21	2.20	2.09

[a]NDVI is normalized difference vegetation index, EVI is enhanced vegetation index, and CI_{green} is green chlorophyll index. PAR_{in} is incident photosynthetically active radiation. *Sims et al.* [2008] give detailed information about the TG model. All the relationships are statistically significant at $p < 0.0001$ ($n = 105$).

the mean LST, which was similar to the results obtained in section 3.1. Further adding EVI to the model depending on mean LST and root zone soil moisture made no obvious improvement at the deciduous forest site in the midgrowing and late-growing periods, which appeared to contradict the results in section 3.1, especially for the midgrowing period. However, the models based on the mean LST, root zone soil moisture, and EVI explained 76% and 90% of the seasonal variation in R_s for midgrowing and late-growing periods, respectively (Table 4), demonstrating the possibility of estimating R_s based on spatial data products at the study site.

3.4. Multicollinearity Diagnostics

In this study, the largest Pearson correlation coefficient among predictive variables used for estimating R_s (i.e., T_{s4}, θ_{10}, GPP, mean LST, root zone soil moisture, and EVI) is 0.78 (Appendix A). Therefore, in accordance to *Hair et al.'s* [1979] criterion that for variables to qualify for multicollinearity should have a coefficient of correlation 0.8 or higher, the problem of multicollinearity does not exist in our data set. The collinearity diagnostics using VIF method also confirmed that multicollinearity was not a problem to distort our regression analysis. The reason was that the highest VIF in our statistical analysis was only 4.32 (Appendix B), a value well within accepted standards [*York et al.*, 2003].

4. Discussion

4.1. Estimating Soil Respiration Using Spatial Data Products at the Deciduous Forest Site

Our results suggested that simple models based entirely on spatial data products have the potential to estimate R_s at the temperate deciduous forest site. This result provides the foundation for the development of R_s models aimed to obtain spatial distributed R_s. However, this approach will need large amounts of soil respiration data to constrain parameters. The same regression coefficients obtained at this study site would not work for other sites with different climate, soil, and vegetation.

Through modeling R_s using biotic and abiotic factors (Table 4), we found that the controlling factors of R_s changed from the growing to nongrowing seasons. Thus, modeling R_s according to phenological periods was necessary, which was consistent with the findings of *Janssens and Pilegaard* [2003] and *Shi et al*. [2006]. During the nongrowing season, the models based on the mean LST and root zone soil moisture, which to some extent tracked the seasonal variations of soil temperature and soil moisture, explained most of the seasonal dynamics of R_s at the deciduous forest site in spring and winter dormant periods with R^2 values of 0.82 and 0.72, respectively.

As the growing season progressed, the contribution of plant photosynthesis to total R_s may increase by enhanced C substrate supply for plant roots and soil microbes in rhizoshpere [*Bahn et al*., 2008; *Martin et al*., 2012; *Moyano et al*., 2007; *Sampson et al*., 2007]. Thus, adding GPP to the model based on T_{s4} and θ_{10} improved the explanatory ability of the R_s model in the early, midgrowing, and late-growing periods (Table 4). When comparing R^2, RMSE, and AIC, the models entirely driven by spatial data products (i.e., mean LST, root zone soil moisture, and photosynthesis-related EVI) showed similar performances to the models based on in situ measured data (T_{s4}, θ_{10}, and GPP) during the growing season, except for the midgrowing period. This suggested that R_s modeling was feasible by using spatially distributed data products.

4.2. Soil Respiration Modeling in the Midgrowing Period

During the midgrowing period, the model based on the in situ measured T_{s4}, θ_{10}, and GPP showed much higher explanation capacity for the seasonal variation of R_s ($R^2 = 0.90$, $p < 0.0001$) than the models based on spatial data products (i.e., mean LST, root zone soil moisture, and EVI; $R^2 = 0.76$, $p < 0.0001$) at the deciduous forest site. The reason may be due to the use of root zone soil moisture instead of surface soil moisture (i.e., θ_{10}) in the modeling of R_s. Surface soil moisture (i.e., θ_{10}) is highly variable because of the influence of atmospheric conditions (rain, wind, and solar radiation), whereas root zone soil moisture presents lower variability than surface soil moisture [*Anguela et al*., 2008; *Rebel et al*., 2012]. For example, θ_{10} had better reaction to precipitation events than other deeper soil moisture and root zone soil moisture at the deciduous forest site (Figure 2). Therefore, using the surface soil moisture (θ_{10}) as a driving factor of R_s may explain more temporal variations in R_s, attributed to the effects of extreme variations in atmospheric conditions, than root zone soil moisture during the midgrowing period. With the occurrence of droughts at the study site in the midgrowing

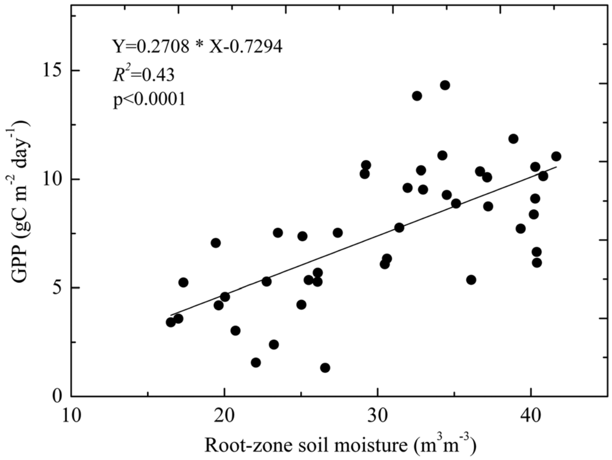

Figure 5. Relationship between root zone soil moisture and gross primary production (GPP) at the temperate deciduous forest site during the midgrowing period of 2004–2007. The data used in this figure is the 8 day mean ($n = 45$).

season [*Gu et al.*, 2006; *Yang et al.*, 2010], precipitation events following droughts often led to unusually large R_s values (Figures 1 and 2). This result may be attributed to the lack of water leading to "bursts" when conditions turned more favorable for root growth and microbial respiration. Similar R_s responses following the precipitation events have also been observed in previous studies [*Fierer and Schimel*, 2003; *Irvine and Law*, 2002; *Misson et al.*, 2006; *Vargas and Allen*, 2008].

We also observed that the inclusion of photosynthesis-related factor (EVI) in the model based on mean LST and root zone soil moisture did not improve the explanation of the seasonal variation in R_s at the study site during the midgrowing period. This insufficiency may be accounted by the direct link between plant photosynthesis and root zone soil moisture during this time period. In vegetated fields, growth and productivity of vegetation is primarily determined by water availability in the root zone [*Rao et al.*, 1993]. Under semiarid or arid conditions, the change of root zone soil moisture can be almost instantaneously reflected by vegetation through biophysical process (e.g., plant photosynthesis) [*Schnur et al.*, 2010; *Wang et al.*, 2007]. However, the capacity of plant photosynthesis to rapidly respond to variations in surface soil moisture is limited under drought conditions, especially at forest sites which can access water in deeper soil [*Farooq et al.*, 2009; *Huang and Fu*, 2000]. In the study area reported in this paper, moderate to severe droughts commonly occur in the midgrowing season [*Gu et al.*, 2006; *Yang et al.*, 2010]. Through regression analysis, we also observed significant correlation between root zone soil moisture and GPP at this deciduous forest site during the midgrowing period ($R^2 = 0.43$, $p < 0.0001$, Figure 5). Therefore, adding photosynthesis-related EVI to the model based on the mean LST and root zone soil moisture did not make an improvement in estimating R_s during the midgrowing period.

4.3. Spatial Scales of Data Used for Estimating Soil Respiration

In this study, the spatial scales of data are widely apart. For example, the spectral vegetation indices and mean LST from MODIS products are at a spatial resolution of 500 m and 1000 m, respectively, while root zone soil moisture is at a spatial resolution of 25 km. As the spatially averaged R_s, soil temperature, and soil moisture represented the observation scale of the flux tower, the MODIS products (i.e, VIs and LST) and in situ measured data (i.e., R_s, soil temperature, soil moisture, and GPP) can be considered to be consistent in spatial scale. The study of *Xiao et al.* [2010] also showed that the spatial scale of MODIS products (500 m and 1000 m) can correspond to the observation scale of eddy flux tower at the Missouri Ozark AmeriFlux site.

The question now was if the coarse-scale root zone soil moisture data (25 km) was a reasonable input for R_s estimation at the observation scale of the flux tower. Root zone soil moisture and measured soil moisture at the flux tower do not necessarily have to agree as they are a result of processes at a different spatial scale. However, despite the differences in spatial scale, both showed consistency in terms of temporal dynamics (e,g., trend) and hence have a similar response to rainfall if the rainfall was equally distributed [*Rebel et al.*, 2012]. The statistical regression analysis also showed that the root zone soil moisture at a coarse scale of 25 km explained the seasonal variations of in situ measured soil moisture, especially for the 40 cm depth soil moisture (Figure 4). In a semiarid region of southwestern USA, soil moisture values of the same depth are highly correlated ($r = 0.53$ to 0.85) among sites as far as 150 km apart [*Schnur et al.*, 2010]. At the Grand Morin watershed (France), *Anguela et al.* [2008] also observed that root zone soil moisture from integrating remotely sensed surface soil moisture observations into a two-layer water model, despite of the 25×25 km^2 scale, produces good quality and is well correlated with soil moisture from in situ time domain reflectometry measurements (local scale) and a hydrological model ($8 \times 8\,km^2$ scale).

5. Conclusions

This study investigated the feasibility of estimating R_s using spatial data products, including mean LST, spectral vegetation index, and root zone soil moisture, at a deciduous forest site located in Midwest USA. Results showed that the models based on mean LST and root zone soil moisture explained most of the nongrowing season (i.e., spring and winter dormant periods) variations in R_s. The models depending on mean LST, root zone soil moisture, and photosynthesis-related EVI showed high accuracy for R_s estimation with R^2 of 0.96 and 0.90 for early and late-growing periods, respectively. During midgrowing period, common occurrence of droughts led to usually large R_s values following precipitation events. Under this condition, surface soil moisture had better response to the extreme variations in R_s than root zone soil moisture during the midgrowing period at the deciduous forest site. Therefore, the model entirely based on spatial data products (i.e., mean LST, root zone soil moisture, and EVI) showed lower explanation capacity ($R^2 = 0.76$ versus $R^2 = 0.90$) for seasonal variation of R_s than the model based on in situ measured data (i.e., T_{s4}, θ_{10}, and GPP). Considering that the factors affecting R_s are complex and diverse at the forest site, including environmental variables, biotic factors, human activities, and site characteristics, the fitting accuracy of the model based on spatial data products during the midgrowing period at the study site is still acceptable. The methodology holds promise for applying spatial data products from remotely sensed observations and the assimilation of remote sensing data into a land surface model to estimate R_s at the regional and global scales. New releases of spatial data products with higher quality and spatial resolution will provide improved R_s estimation that can be used to enhance the global assessments of carbon budgets.

Appendix A: Pearson's Correlation Coefficient

Tables A1 and A2 described the results of multicollinearity diagnostics for the predictive variables used for estimating soil respiration (R_s) at the temperate deciduous forest site from 2004 to 2007 at five different phenological periods. The largest Pearson correlation coefficient among the predictive variables used for estimating R_s is 0.78. Therefore, in accordance to *Hair et al.*'s [1979] criterion that for variables to qualify for multicollinearity should have a coefficient of correlation 0.8 or higher, the problem of multicollinearity does not exist in our data set.

Table A1. Pearson Correlation Coefficient (r) Among Soil Temperature at 4 cm Depth (T_{s4}, °C), Soil Moisture at 10 cm Depth (θ_{10}, m^3m^{-3}), and Gross Primary Production (GPP, gC m^{-2} day^{-1}) at the Temperate Deciduous Forest Site From 2004 to 2007 at Five Different Phenological Periods

	Spring Dormant Period		Early Growing Period			Midgrowing Period			Late-Growing Period			Winter Dormant Period	
	T_{s4}	θ_{10}	T_{s4}	θ_{10}	GPP	T_{s4}	θ_{10}	GPP	T_{s4}	θ_{10}	GPP	T_{s4}	θ_{10}
T_{s4}	1.00		1.00			1.00			1.00			1.00	
θ_{10}	−0.16	1.00	−0.16	1.00		−0.38	1.00		−0.76	1.00		0.33	1.00
GPP			0.65	−0.50	1.00	0.23	−0.07	1.00	0.55	−0.35	1.00		

Table A2. Pearson Correlation Coefficient (r) Among Averaged Daytime and Nighttime Land Surface Temperature (Mean LST, °C) From Terra MODIS, Root Zone Soil Moisture (θ_r, m^3 m^{-3}), and Enhanced Vegetation Index (EVI) at the Temperate Deciduous Forest Site From 2004 to 2007 at Five Different Phenological Periods

	Spring Dormant Period		Early Growing Period			Midgrowing Period			Late-Growing Period			Winter Dormant Period	
	Mean LST	θ_r	Mean LST	θ_r	EVI	Mean LST	θ_r	EVI	Mean LST	θ_r	EVI	Mean LST	θ_r
Mean LST	1.00		1.00			1.00			1.00			1.00	
θ_r	0.02	1.00	−0.56	1.00		−0.22	1.00		−0.43	1.00		−0.41	1.00
EVI			0.71	−0.58	1.00	0.71	0.26	1.00	0.78	−0.11	1.00		

Table B1. Variance Inflation Factor (VIF) for the Predictive Variables in Soil Respiration Estimation at the Temperate Deciduous Forest Site From 2004 to 2007 at Five Different Phenological Periods[a]

Model	Predictive Variables	Spring Dormant Period	Early Growing Period	Midgrowing Period	Late-Growing Period	Winter Dormant Period
1	T_{s4}	1.03	1.03	1.16	2.39	1.12
	θ_{10}	1.03	1.03	1.16	2.39	1.12
2	T_{s4}		1.82	1.22	3.06	
	θ_{10}		1.41	1.16	2.43	
	GPP		2.35	1.06	1.46	

[a]In models 1 and 2, soil respiration (R_s, μmol CO_2 m^{-2} s^{-1}) is dependent variable. Using the multicollinearity diagnosis in SPSS software, we calculated the variance inflation factor (VIF) for predictive variables in models 1 and 2, respectively. T_{s4} is soil temperature at 4 cm depth (°C), θ_{10} is volumetric soil moisture (m^3 m^{-3}) at 10 cm depth, and GPP is gross primary production (gC m^{-2} day^{-1}). T_{s4} and θ_{10} are predictive variables for model 1. T_{s4}, θ_{10}, and GPP are predictive variables for model 2.

Table B2. Variance Inflation Factor (VIF) for the Predictive Variables in Soil Respiration Estimation at the Temperate Deciduous Forest Site From 2004 to 2007 at Five Different Phenological Periods[a]

Model	Predictive Variables	Spring Dormant Period	Early Growing Period	Midgrowing Period	Late-Growing Period	Winter Dormant Period
1	Mean LST	1.00	1.46	1.05	1.22	1.20
	θ_r	1.00	1.46	1.05	1.22	1.20
2	Mean LST		2.18	3.14	4.32	
	θ_r		1.63	1.67	1.71	
	EVI		2.26	3.20	3.38	

[a]In models 1 and 2, soil respiration (R_s, μmol CO_2 m^{-2} s^{-1}) is dependent variable. Using the multicollinearity diagnosis in SPSS software, we calculated the variance inflation factor (VIF) for predictive variables in models 1 and 2, respectively. Mean LST is the averaged daytime and nighttime land surface temperature (LST) from Terra MODIS (°C), θ_r is the root zone soil moisture (m^3 m^{-3}), and EVI is the enhanced vegetation index for estimating gross primary production (GPP, gC m^{-2} day^{-1}). Mean LST and θ_r are predictive variables for model 1. Mean LST, θ_r, and EVI are predictive variables for model 2.

Appendix B: Variance Inflation Factor

Tables B1 and B2 described the results of multicollinearity diagnostics for the predictive variables used for estimating soil respiration (R_s) at the temperate deciduous forest site from 2004 to 2007 at five different phenological periods. The collinearity diagnostics using VIF method also confirmed that multicollinearity was not a problem to distort our regression analysis. The reason was that the highest VIF in our statistical analysis was only 4.32, a value well within accepted standards [*York et al.*, 2003].

Acknowledgments
We sincerely thank the anonymous reviewers for their important and constructive revision advices on the manuscript. We like to offer thanks to the America Fluxnet (http://public.ornl.gov/ameriflux/) which provides the data for our analysis. We also thank B. Yang from Environmental Sciences Division, Oak Ridge National Laboratory, Oak Ridge, Tennessee, USA, for useful suggestions about the use of soil CO_2 flux data, and J.D. Bolten from Hydrological Sciences Branch, NASA Goddard Space Flight Center, Beltsville, MD, for helpful explanation about the root zone soil moisture product. This work was supported by the National Natural Science Foundation of China (41301498), the Special Foundation for Young Scientists of the State Laboratory of Remote Sensing Science (13RC-07), and the Major State Basic Research Development Program of China (2013CB733405).

References

Amos, B., T. J. Arkebauer, and J. W. Doran (2005), Soil surface fluxes of greenhouse gases in an irrigated maize-based agroecosystem, *Soil Sci. Soc. Am. J.*, *69*, 387–395.

Anguela, T. P., M. Zribi, S. Hasenauer, F. Habets, and C. Loumagne (2008), Analysis of surface and root-zone soil moisture dynamics with ERS scatterometer and the hydrometeorological model SAFRAN-ISBA-MODCOU at Grand Morin watershed (France), *Hydrol. Earth Syst. Sci.*, *12*, 1415–1424.

Arkebauer, T. J., E. A. Walter-Shea, M. A. Mesarch, A. E. Suker, and S. B. Verma (2009), Scaling up of CO_2 fluxes from leaf to canopy in maize-based agroecosystems, *Agric. For. Meteorol.*, *149*, 2110–2119.

Bahn, M., et al. (2008), Soil respiration in European grasslands in relation to climate and assimilate supply, *Ecosystems*, *11*, 1352–1367.

Balogh, J., K. Pinter, S. Foti, D. Cserhalmi, M. Papp, and Z. Nagy (2011), Dependence of soil respiration on soil moisture, clay content, soil organic matter, and CO_2 uptake in dry grasslands, *Soil Biol. Biochem.*, *43*, 1006–1013.

Benali, A., A. C. Carvalho, J. P. Nunes, N. Carvalhais, and A. Santos (2012), Estimating air surface temperature in Portugal using MODIS LST data, *Remote Sens. Environ.*, *124*, 108–121.

Bolten, J. D., V. Lakshmi, and E. G. Njoku (2003), Soil moisture retrieval using the passive/active L- and S-band radar/radiometer, *IEEE Trans. Geosci. Remote Sens.*, *41*, 2792–2801.

Bolten, J. D., W. T. Crow, X. W. Zhan, T. J. Jackson, and C. A. Reynolds (2010), Evaluating the utility of remotely sensed soil moisture retrievals for operational agricultural drought monitoring, *IEEE J. Sel. Topics Appl. Earth Observ. Remote Sens.*, *3*, 57–66.

Chen, J., P. Jonsson, M. Tamura, Z. H. Gu, B. Matsushita, and L. Eklundh (2004), A simple method for reconstructing a high-quality NDVI time-series data set based on the Savitzky–Golay filter, *Remote Sens. Environ.*, *91*, 3–4.

Cook, F. J., and V. A. Orchard (2008), Relationships between soil respiration and soil moisture, *Soil Biol. Biochem.*, *40*, 1013–1018.

Cosh, M. H., T. J. Jackson, R. Bindlish, and J. H. Prueger (2004), Watershed scale temporal and spatial stability of soil moisture and its role in validating satellite estimates, *Remote Sens. Environ.*, *92*, 427–435.

Davidson, E. A., E. Belk, and R. D. Boone (1998), Soil water content and temperature as independent or confound factors controlling soil respiration in a temperature mixed hardwood forest, *Global Change Biol.*, *4*, 217–227.

Davidson, E. A., A. D. Richardson, K. E. Savage, and D. Y. Hollinger (2006), A distinct seasonal pattern of the ratio of soil respiration to total ecosystem respiration in a spruce-dominated forest, *Global Change Biol.*, *12*, 230–239.

Edwards, N. T., and J. S. Riggs (2003), Automated monitoring of soil respiration: A moving chamber design, *Soil Sci. Soc. Am. J.*, *67*, 1266–1271.

Famiglietti, J. S., D. Ryu, A. Berg, M. Rodell, and T. J. Jackson (2008), Field observations of soil moisture variability across scales, *Water Resour. Res.*, *44*, W01423, doi:10.1029/2006WR005804.

Fang, H., S. Liang, M. Chen, C. Walthall, and C. Daughtry (2004), Statistical comparison of MISR, ETM plus and MODIS land surface reflectance and albedo products of the BARC land validation core site USA, *Int. J. Remote Sens.*, *25*, 409–422.

Farooq, M., A. Wahid, N. Kobayashi, D. Fujita, and S. M. A. Basra (2009), Plant drought stress: Effects, mechanisms and management, *Agron. Sustainable Dev.*, *29*, 185–212.

Fierer, N., and J. P. Schimel (2003), A proposed mechanism for the pulse in carbon dioxide production commonly observed following the rapid rewetting of a dry soil, *Soil Sci. Soc. Am. J.*, *67*, 798–805.

Gamon, J. A., C. B. Field, M. L. Goulden, K. L. Griffin, A. E. Hartley, G. Joel, J. Peñuelas, and R. Valentini (1995), Relationship between NDVI, canopy structure and photosynthesis in three Californian vegetation types, *Ecol. Appl.*, *5*, 28–41.

Ganguly, S., M. A. Friedl, B. Tan, X. Y. Zhang, and M. Verma (2010), Land surface phenology from MODIS: Characterization of the Collection 5 global land cover dynamics product, *Remote Sens. Environ.*, *114*, 1805–1816.

Gaumont-Guay, D., T. A. Black, T. J. Griffis, A. G. Barr, R. S. Jassal, and Z. Nesic (2006), Interpreting the dependence of soil respiration on soil temperature and water content in a boreal aspen stand, *Agric. For. Meteorol.*, *140*, 220–235.

Gitelson, A. A., A. Vina, V. Ciganda, D. C. Rundquist, and T. J. Arkebauer (2005), Remote estimation of canopy chlorophyll content in crops, *Geophys. Res. Lett.*, *32*, L08403, doi:10.1029/2005GL022688.

Gitelson, A. A., A. Vina, S. B. Verma, D. C. Rundquist, T. J. Arkebauer, G. Keydan, B. Leavitt, V. Ciganda, G. G. Burba, and A. E. Suyker (2006), Relationship between gross primary production and chlorophyll content in crops: Implications for the synoptic monitoring of vegetation productivity, *J. Geophys. Res.*, *111*, D08S11, doi:10.1029/2005JD006017.

Gu, L., W. M. Post, and A. W. King (2004), Fast labile carbon turnover obscures sensitivity of heterotrophic respiration from soil to temperature: A model analysis, *Global Biogeochem. Cycles*, *18*, GB1022, doi:10.1029/2003GB002119.

Gu, L. H., T. Meyers, S. G. Pallardy, P. J. Hanson, B. Yang, M. Heuer, K. P. Hosman, J. S. Riggs, D. Sluss, and S. D. Wullschleger (2006), Direct and indirect effects of atmospheric conditions and soil moisture on surface energy partitioning revealed by a prolonged drought at a temperate forest site, *J. Geophys. Res.*, *111*, D16102, doi:10.1029/2006JD007161.

Gu, L. H., P. J. Hanson, W. Mac Post, and Q. Liu (2008), A novel approach for identifying the true temperature sensitivity from soil respiration measurements, *Global Biogeochem. Cycles*, *22*, GB4009, doi:10.1029/2007GB003164.

Hair, J. F., R. E. Anderson, R. L. Tatham, and B. J. Grablowsky (1979), *Multivariate Data Analysis*, Petroleum Publishing Company, Tulsa, OK.

Han, G. X., G. S. Zhou, Z. Z. Xu, Y. Yang, J. L. Liu, and K. Q. Shi (2007), Biotic and abiotic factors controlling the spatial and temporal variation of soil respiration in an agricultural ecosystem, *Soil Biol. Biochem.*, *39*, 418–425.

Högberg, P., A. Nordgren, N. Buchmann, A. F. S. Taylor, A. Ekblad, M. N. Högberg, G. Nyberg, M. Ottosson-Lofvenius, and D. J. Read (2001), Large-scale forest girdling shows that current photosynthesis drives soil respiration, *Nature*, *411*, 789–792.

Houser, P. R., W. J. Shuttleworth, J. S. Famiglietti, H. V. Gupta, K. H. Syed, and D. C. Goodrich (1998), Integration of soil moisture remote sensing and hydrologic modeling using data assimilation, *Water Resour. Res.*, *34*, 3405–3420.

Huang, B. R., and J. M. Fu (2000), Photosynthesis, respiration, and carbon allocation of two cool-season perennial grasses in response to surface soil drying, *Plant Soil*, *227*, 17–26.

Huang, C. L., X. Li, and L. Lu (2008), Retrieving soil temperature profile by assimilating MODIS LST products with ensemble Kalman filter, *Remote Sens. Environ.*, *112*, 1320–1336.

Huete, A., K. Didan, T. Miura, E. P. Rodriguez, X. Cao, and L. G. Ferreira (2002), Overview of the radiometric and biophysical performance of the MODIS vegetation indices, *Remote Sens. Environ.*, *83*, 195–213.

Hulley, G. C., and S. J. Hook (2009), Intercomparison of versions 4, 4.1 and 5 of the MODIS Land Surface Temperature and Emissivity products and validation with laboratory measurements of sand samples from the Namib desert, Namibia, *Remote Sens. Environ.*, *113*, 1313–1318.

Irvine, J., and B. E. Law (2002), Contrasting soil respiration in young and old-growth ponderosa pine forests, *Global Change Biol.*, *8*, 1183–1194.

Janssens, I. A., and K. Pilegaard (2003), Large seasonal changes in Q_{10} of soil respiration in a beech forest, *Global Change Biol.*, *9*, 911–918.

Jassal, R. S., T. A. Black, M. D. Novak, D. Gaumont-Guay, and Z. Nesic (2008), Effect of soil water stress on soil respiration and its temperature sensitivity in an 18-year-old temperate Douglas-fir stand, *Global Change Biol.*, *14*, 1305–1318.

Jin, M. L., and R. E. Dickinson (2010), Land surface skin temperature climatology: Benefitting from the strengths of satellite observations, *Environ. Res. Lett. 5*, 044004, doi:10.1088/1748-9326/5/4/044004.

Kimball, J. S., L. A. Jones, K. Zhang, F. A. Heinsch, K. C. McDonald, and W. C. Oechel (2009), A satellite approach to estimate land-atmosphere CO_2 exchange for boreal and arctic biomes using MODIS and AMSR-E, *IEEE Trans. Geosci. Remote Sens.*, *47*, 569–587.

Kuzyakov, Y., and O. Richkovaw (2010), Time lag between photosynthesis and carbon dioxide efflux from soil: A review of mechanisms and controls, *Global Change Biol.*, *16*, 3386–3406.

Li, H. J., J. X. Yan, X. F. Yue, and M. B. Wang (2008), Significance of soil temperature and moisture for soil respiration in a Chinese mountain area, *Agric. For. Meteorol.*, *148*, 490–503.

Liang, S. L., H. L. Fang, M. Z. Chen, C. J. Shuey, C. Walthall, C. Daughtry, J. Morisette, C. Schaaf, and A. Strahler (2002), Validating MODIS land surface reflectance and albedo products: Methods and preliminary results, *Remote Sens. Environ.*, *83*, 149–162.

Liu, Q., N. T. Edwards, W. M. Post, L. Gu, J. Ledford, and S. Lenhart (2006), Temperature-independent diel variation in soil respiration observed from a temperate deciduous forest, *Global Change Biol.*, *12*, 2136–2145.

Lloyd, J., and J. A. Taylor (1994), On the temperature dependence of soil respiration, *Funct. Ecol.*, *8*, 315–323.

Martin, J. G., C. L. Phillips, A. Schmidt, J. Irvine, and B. E. Law (2012), High-frequency analysis of the complex linkage between soil CO_2 fluxes, photosynthesis and environmental variables, *Tree Physiol.*, *32*, 49–64.

Migliavacca, M., et al. (2011), Semiempirical modeling of abiotic and biotic factors controlling ecosystem respiration across eddy covariance sites, *Global Change Biol.*, *17*, 390–409.

Misson, L., A. Gershenson, J. W. Tang, M. McKay, W. X. Cheng, and A. Goldstein (2006), Influences of canopy photosynthesis and summer rain pulses on root dynamics and soil respiration in a young ponderosa pine forest, *Tree Physiol.*, *26*, 833–844.

Moncet, J. L., P. Liang, A. E. Lipton, J. F. Galantowicz, and C. Prigent (2011), Discrepancies between MODIS and ISCCP land surface temperature products analyzed with microwave measurements, *J. Geophys. Res.*, *116*, D21105, doi:10.1029/2010JD015432.

Mostovoy, G. V., R. L. King, K. R. Reddy, V. G. Kakani, and M. G. Filippova (2006), Statistical estimation of daily maximum and minimum air temperatures from MODIS LST data over the state of Mississippi, *GISci. Remote Sens.*, *43*, 78–110.

Moyano, F. E., W. L. Kutsch, and E. D. Schulze (2007), Response of mycorrhizal, rhizosphere and soil basal respiration to temperature and photosynthesis in a barley field, *Soil Biol. Biochem.*, *39*, 843–853.

Njoku, E., and S. K. Chan (2006), Vegetation and surface roughness effects on AMSR-E land observations, *Remote Sens. Environ.*, *100*, 190–199.

Oyonarte, C., A. Rey, J. Raimundo, I. Miralles, and P. Escribano (2012), The use of soil respiration as an ecological indicator in arid ecosystems of the SE of Spain: Spatial variability and controlling factors, *Ecol. Indic.*, *14*, 40–49.

Pallardy, S. G., T. A. Nigh, and H. E. Garrett (1988), Changes in forest composition in central Missouri: 1968–1982, *Am. Midland Nat.*, *120*, 380–390.

Peng, Y., and A. A. Gitelson (2011), Application of chlorophyll-related vegetation indices for remote estimation of maize productivity, *Agric. For. Meteorol.*, *151*, 1267–1276.

Rahman, A. F., D. A. Sims, V. D. Cordova, and B. Z. El-Masri (2005), Potential of MODIS EVI and surface temperature for directly estimating per-pixel ecosystem C fluxes, *Geophys. Res. Lett.*, *32*, L19404, doi:10.1029/2005GL024127.

Rao, P. V. N., L. Venkataratnam, P. V. K. Rao, K. V. Ramana, and M. N. Singarao (1993), Relation between root zone soil moisture and normalized difference vegetation index of vegetated fields, *Int. J. Remote Sens.*, *14*, 441–449.

Rebel, K. T., R. A. M. de Jeu, P. Ciais, N. Viovy, S. L. Piao, G. Kiely, and A. J. Dolman (2012), A global analysis of soil moisture derived from satellite observations and a land surface model, *Hydrol. Earth.Syst. Sci.*, *16*, 833–847.

Reichstein, M., et al. (2003), Modeling temporal and large-scale spatial variability of soil respiration from soil water availability, temperature and vegetation productivity indices, *Global Biogeochem. Cycles*, *17*(4), 1104, doi:10.1029/2003GB002035.

Reichstein, M., et al. (2005), On the separation of net ecosystem exchange into assimilation and ecosystem respiration: Review and improved algorithm, *Global Change Biol.*, *11*, 1424–1439.

Richardson, A. D., et al. (2006), Comparing simple respiration models for eddy flux and dynamic chamber data, *Agric. For. Meteorol.*, *141*, 219–234.

Rouse, J. W., R. H. Haas, J. A. Schell, D. W. Deering, and J. C. Harlan (1974), Monitoring the vernal advancements and retrogradation of natural vegetation, final report, pp. 1–137, NASA/GSFC, Greenbelt, MD.

Running, S. W., P. E. Thornton, R. R. Nemani, and J. M. Glassy (2000), Global terrestrial gross and net primary productivity from the Earth observing system, in *Methods in Ecosystem Science*, edited by O. Sala et al., pp. 44–57, Springer, New York.

Ryan, M. G., and B. E. Law (2005), Interpreting, measuring, and modeling soil respiration, *Biogeochemistry*, *73*, 3–27.

Sampson, D. A., I. A. Janssens, J. C. Yuste, and R. Ceulemans (2007), Basal rates of soil respiration are correlated with photosynthesis in a mixed temperate forest, *Global Change Biol.*, *13*, 2008–2017.

Savitzky, A., and M. J. E. Golay (1964), Smoothing and differentiation of data by simplified least squares procedures, *Anal. Chem.*, *36*, 1627–1639.

Schnur, M. T., H. J. Xie, and X. W. Wang (2010), Estimating root zone soil moisture at distant sites using MODIS NDVI and EVI in a semi-arid region of southwestern USA, *Ecol. Inf.*, *5*, 400–409.

Shi, P. L., X. Z. Zhang, Z. M. Zhong, and H. Ouyang (2006), Diurnal and seasonal variability of soil CO2 efflux in a cropland ecosystem on the Tibetan Plateau, *Agric. For. Meteorol.*, *137*, 220–233.

Sims, D. A., et al. (2006), On the use of MODIS EVI to assess gross primary productivity of North American ecosystems, *J. Geophys. Res.*, *111*, G04015, doi:10.1029/2006JG000162.

Sims, D. A., et al. (2008), A new model of gross primary productivity for North American ecosystems based solely on the enhanced vegetation index and land surface temperature from MODIS, *Remote Sens. Environ.*, *112*, 1633–1646.

Tang, J. W., D. D. Baldocchi, and L. Xu (2005a), Tree photosynthesis modulates soil respiration on a diurnal time scale, *Global Change Biol.*, *11*, 1298–1304.

Tang, J. W., L. Misson, A. Gershenson, W. X. Cheng, and A. H. Goldstein (2005b), Continuous measurements of soil respiration with and without roots in a ponderosa pine plantation in the Sierra Nevada Mountains, *Agric. For. Meteorol.*, *132*, 212–227.

Vargas, R., and M. F. Allen (2008), Environmental controls and the influence of vegetation type, fine roots and rhizomorphs on diel and seasonal variation in soil respiration, *New Phytol.*, *179*, 460–471.

Vargas, R., et al. (2010), Looking deeper into the soil: Biophysical controls and seasonal lags of soil CO_2 production and efflux, *Ecol. Appl.*, *20*, 1569–1582.

Vargas, R., M. S. Carbone, M. Reichstein, and D. D. Baldocchi (2011), Frontiers and challenges in soil respiration research: From measurements to model-data integration, *Biogeochemistry*, *102*, 1–13.

Verstraeten, W. W., F. Veroustraete, C. J. van der Sande, I. Grootaers, and J. Feyen (2006), Soil moisture retrieval using thermal inertia, determined with visible and thermal spaceborne data, validated for European forests, *Remote Sens. Environ.*, *101*, 299–314.

Vogt, J. V., A. A. Viau, and F. Paquet (1997), Mapping regional air temperature fields using satellite-derived surface skin temperatures, *Int. J. Climatol.*, *17*, 1559–1579.

von Deimling, T. S., M. Meinshausen, A. Levermann, V. Huber, K. Frieler, D. M. Lawrence, and V. Brovkin (2012), Estimating the near-surface permafrost-carbon feedback on global warming, *Biogeosciences*, *9*, 649–665.

Wan, Z. M. (2008), New refinements and validation of the MODIS Land-Surface Temperature/Emissivity products, *Remote Sens. Environ.*, *112*, 59–74.

Wang, X. W., H. J. Xie, H. D. Guan, and X. B. Zhou (2007), Different responses of MODIS-derived NDVI to root-zone soil moisture in semi-arid and humid regions, *J. Hydrol.*, *340*, 12–24.

Wu, C., Z. Niu, and S. Gao (2010), Gross primary production estimation from MODIS data with vegetation index and photosynthetically active radiation in maize, *J. Geophys. Res.*, *115*, D12127, doi:10.1029/2009JD013023.

Wylie, B. K., D. A. Johnson, E. Laca, N. Z. Saliendra, T. G. Gilmanov, B. C. Reed, L. L. Tieszen, and B. B. Worstell (2003), Calibration of remotely sensed, coarse resolution NDVI to CO_2 fluxes in a sagebrush-steppe ecosystem, *Remote Sens. Environ.*, *85*, 243–255.

Xiao, J. F., et al. (2010), A continuous measure of gross primary production for the conterminous United States derived from MODIS and AmeriFlux data, *Remote Sens. Environ.*, *114*, 576–591.

Xiao, X., D. Hollinger, J. Aber, M. Gholtz, E. A. Davidson, Q. Zhang, and B. Moore III (2004), Satellite-based modeling of gross primary production in an evergreen needleleaf forest, *Remote Sens. Environ.*, *89*, 519–534.

Yang, B., S. G. Pallardy, T. P. Meyers, L. H. Gu, P. J. Hanson, S. D. Wullschleger, M. Heuer, K. P. Hosman, J. S. Riggs, and D. W. Sluss (2010), Environmental controls on water use efficiency during severe drought in an Ozark Forest in Missouri USA, *Global Change Biol.*, *16*, 2252–2271.

York, R., E. A. Rosa, and T. Dietz (2003), STIRPAT, IPAT and ImPACT: Analytic tools for unpacking the driving forces of environmental impacts, *Ecol. Econ.*, *46*, 351–365.

Zhang, W., Y. Huang, Y. Q. Yu, and W. J. Sun (2011), Empirical models for estimating daily maximum, minimum and mean air temperatures with MODIS land surface temperatures, *Int. J. Remote Sens.*, *32*, 9415–9440.